JSEE Vol. 22, No. 1, 2020 DOI:10.48303/jsee.2020.245117

Estimation of Seismic Hazard and Amplification of Strong Ground Motions in Indo-Gangetic Plains

Priyanka Sharma[1], Mukat Lal Sharma[2], and Viswas A. Sawant[3]*

1. Research Scholar, Department of Earthquake Engineering, IIT Roorkee, Roorkee-247667, India, *Corresponding Author; email: pssharma.iitr@gmail.com
2. Professor, Department of Earthquake Engineering, IIT Roorkee, Roorkee-24766, India
3. Professor, Department of Civil Engineering, IIT Roorkee, Roorkee-247667, India

Received: 09/01/2020
Accepted: 27/07/2021

ABSTRACT

In India, many regions under high seismic risk are located on deep soil deposits extending up to several hundred meters of depth. Deep sedimentary deposits are more prone to earthquake hazard. The Indo-Gangetic Basin (IGB) is located in the vicinity of Himalayan Frontal Fault (HFT) and the presence of thick alluvium makes it more vulnerable to seismogenic sources and hence, its characterization is required. In the present study, six sites in Uttarakhand are characterized by using the joint fit Inversion method from the data obtained from Multi Channel Analysis of Surface Waves (MASW) technique with a combination of Horizontal-to-Vertical Curve (H/V) from microtremor studies. Further, seismic hazard assessment for a scenario earthquake (M_w= 8.0) is performed to study the behavior of IGB. There is an increase in spectral acceleration at sites with deep soil profiles and amplification also increases due to the presence of deep soil deposits in this region. This indicates that these sites suffer from high liquefaction potential as compared to shallow soil profiles. Moreover, peak ground horizontal accelerations at bedrock level are computed by dividing the study area into seven seismogenic source zones. On a regional scale, the b value is relatively high for seismic zone VI indicating high locally concentrated stress and fracturing. Also, the value of λ is highest in seismic zone IV and lowest in seismic zone II. The estimated return periods for $R_{6.0}$, $R_{7.0}$ and $R_{8.0}$, represents the seismic zone IV as the most active in the whole region. The estimated hazard parameters are possibly in agreement with the reported hazard parameters in the literature. Seismic characteristics of seismogenic source zones may be used for earthquake engineering purposes, e.g. assigning the severity of input motions for earthquake resistant construction.

Keywords:
Deep Soil; MASW; H/V; Seismogenic Source Zone; Amplification

1. Introduction

About 59% of India's land mass is at a risk of moderate to high seismic hazard covering many important cities, as given in seismic zoning of the country. The existence of fertile soil and water has led to the development of civilizations around river soil deposits, especially near mountains. These areas are more susceptible to damage, in occurrence of seismic activity, due to local site effects. In addition, the rapid growth of the world's population in recent decades has resulted in the construction of many buildings and infrastructure in urban areas on deep soil deposits. Thus, the increase in development of urban areas on deep soil deposits is posing a great threat to seismic hazard. The recently experienced large earthquakes caused heavy damage at epicentral distances ranging from 250-500 km or so due to local site conditions. For example, in 1985 Mexico earthquake, major damage was observed at 200 miles

away from the epicenter in Mexico City. Similarly, in Bhuj earthquake, 2001, heavy damage was seen in multistory building at an epicentral distance of 350 km in Ahmedabad City. Hence, it becomes important to accurately estimate seismic hazard and provide earthquake-resistant structural design to withstand any future earthquake and to minimize the vulnerability of economic and human losses in such areas.

The Indo-Gangetic Basin (IGB) lies parallel to the Himalayas and is highly populated. The basin is formed by the loose soil deposits and any future earthquake in the Himalayas will lead to massive destruction and will pose a threat to both life and property. It is generally referred to as deep soil if the soil cover extends under 30 m from the ground surface. Seismic site response is usually performed considering top 30 m of soil cover. Due to the occurrence of small to large earthquakes, areas underlined by deep soil deposits often suffer a large-scale loss of structure and lives. Several studies [1-3] conducted on Indian soils where only top 30 m of soil cover is considered. Deep soil studies that take full soil thickness into account are very scarce. Luke et al. [4] investigated deep dry sandy soil seismic response and found that the amplitude of acceleration decreased and the predominant period increased with depth. Ashford et al. [5] presents the results of a study in Bangkok on the amplification of strong ground motions that concluded that the soil have the potential to amplify ground motion up to five times the input motion. Anbazhagan and Sitharam [6] studied the spatial variability of the weathered and engineering bedrock using geophysical methods and incorporating the local site effects. Huang et al. [7] provided a seismic site response study of Shanghai's deep saturated soil using constitutive modeling and capturing the deep saturated soil's fundamental seismic aspects. Chen et al. [8] also studied the response of deep Shanghai soil for earthquake loading. Jakka et al. [9] studied the effect of soil cover and the influence of soil type on deep soil response. The site response study for Delhi region was done by Kumar et al. [10]. Hence, it becomes necessary to consider these local site conditions in order to predict the seismic hazard before the occurrence of an earthquake and proper mitigations measures can be taken for the infrastructures.

In the present study, the region selected for site characterization is Indo-Gangetic Basin attributing to its high seismicity and having local site characteristics of soil. Six important sites, namely, Roorkee, Kashipur, UdhamSingh Nagar, Khatima, Haldwani and Kotdwar are selected in the state of Uttarakhand lying in seismic Zone IV (IS: 1893-Part I [11]) for seismic site characterization. The shear wave velocity is estimated up to 500 m in depth using the joint fit inversion technique from dispersion curves obtained from multichannel analysis of surface wave (MASW) and horizontal to vertical spectral ratio curves from microtremor measurements using Nakamura's method [12]. Secondly, seismic hazard is estimated for scenario earthquakes of $M_w = 8.0$ occurring in the proximity of Himalayan Frontal Fault using NGA-West 2 GMPEs and the amplification of strong ground motion is quantified due to deep soil effects. Thirdly, the fundamental aspects of the impact of deep soil effects on strong ground motion are explored.

2. Seismotectonic of Himalayas

The ongoing interaction of the continental plates of India Eurasia has given rise to Tibetan Plateau and the mighty Himalayas. It is a classic example of tectonic collision and draws scientists to consider orogenic cycles, global climate change, and tectonic processes. The Himalayan mountain range falls geographically between the eastern and western Himalayan syntaxes. Geologically, the Himalayan arc consists of Higher Himalayas, Lesser Himalayas and Outer Himalayas longitudinal zones running from north to south over a 2900 km distance. Higher Himalayas consists of crystalline and metamorphic rocks, while, Lesser Himalayas consists of Precambrian sequences and Outer Himalayas consists of fluvial sediments. In the southern sides, all these longitudinal zones are bounded by Main Boundary Thrust (MBT), Main Central Thrust (MCT) and Himalayan Frontal Thrust (HFT) respectively (Figure 1). The western (Kashmir, Zanskar, Spiti, Himachal, Garhwal Kumaun), central (Nepal, Sikkim, and south-central Tibet) and eastern (Bhutan, Arunachal, and southeastern Tibet) segments form the broad main divisions of the Himalayan region [13]. Recent data on seismicity in the region have also shown high seismicity. It is assumed that the convergence of the plates took place at a high rate of about 10 cm/year before 30-

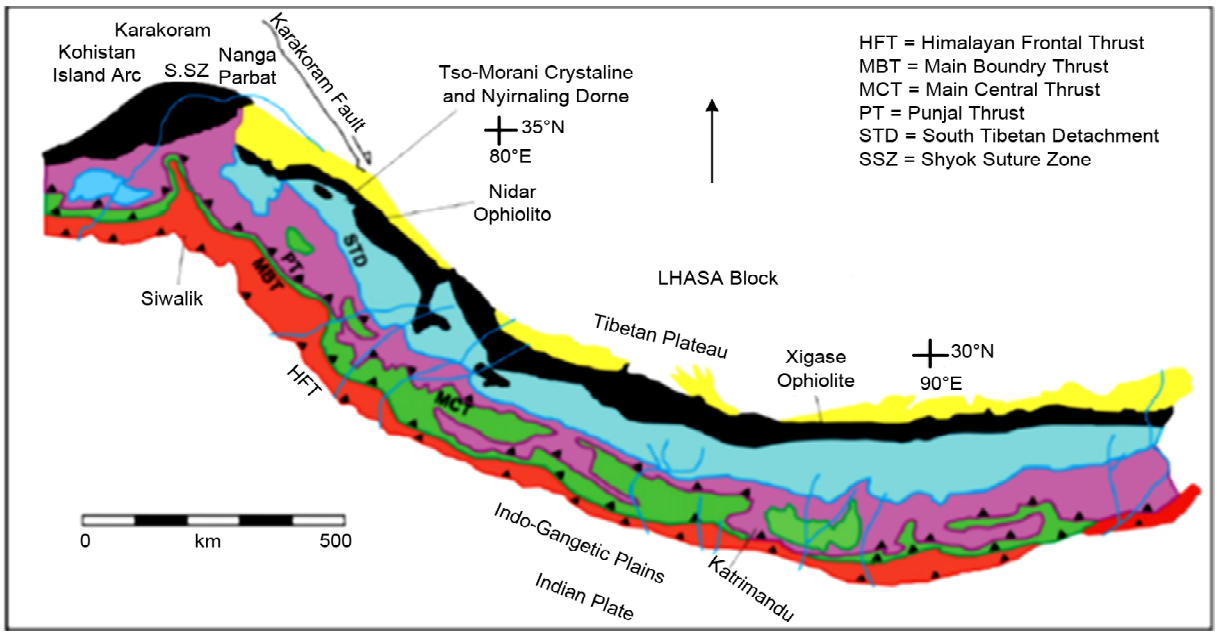

Figure 1. Prominent tectonic features and geology of the Himalayan arc [18].

45 million years BP. A large part of this convergence occurred by thrusting along the Himalayan frontal zone, while components of the remaining movement were distributed across wider tectonic regions including the Pamirs and the Tibetan plateau. Moreover, from the literature, it is believed that thrusting along the Himalayan frontal zone took place 40-45 million year BP. The suture eventually became inactive and since around 25 million years BP, the Main Central Thrust (MCT) took up the convergence movement. According to GPS measurements, the convergence level of India in northeast is 55 mm/year, out of which 18-22 mm/year is accommodated within the Himalayas [14]. The Himalayan geology and tectonics in view of its high seismicity has been explored by many researchers such as Teotia et al. [15], Kumar and Mahajan [16], Sharma and Lindholm [17] etc. India's ongoing northern convergence induces significant deformation in the Himalayas, Tibet, and neighboring regions, thus, making the whole region seismically active.

3. Significant Earthqaukes in Himalayan Region

Over the past 120 years, the Himalayan mountain arc and the neighboring Shillong plateau and western Assam have witnessed four major ($Mw \geq 8.0$ magnitude) earthquakes, namely, Western Assam earthquake (1897), Kangra earthquake (1905), Bihar-Nepal earthquake (1934) and Eastern Assam earthquake (1950) (Figure 2). The great Shillong earthquake of 1897 (Ms = 8.7) was the first event recorded instrumentally by a few stations outside the country. The earthquake experienced peak ground acceleration of more than 1 g with maximum intensity reported as X-XII (MM Scale) caused heavy damage in the vicinity of epicenter. The Kangra earthquake of 1905 (Ms = 7.8) occurred in the HFT zone in the western Himalayas caused severe destruction in the Kangra valley with a maximum intensity X (MM scale). Also, about 250 km south-east, near Dehradun, an isolated intensity VIII (MM scale) was reported with depth of focus at 21-40 km [19]. Further, an aftershock of Ms = 7.0 occurred near Dehradun after few minutes of main shock at a depth of 30-35 km. The Bihar earthquake of 1934 (Ms = 8.4) has its epicenter approximately 50 km south of the MBT and depth at 30 km [20-21]. Maximum intensity X (MM scale) was reported in Munger, Bihar (south of MBT) and a smaller area in Kathmandu, Nepal (north of MBT). The great Assam earthquake of 1950 (Ms = 8.7) occurred after sixteen years of the great Bihar earthquake of 1934 occurred in the eastern syntax area where the N - S Burmese arc meets the E-W Himalayan arc. The maximum intensity XII (MM scale) and focal depth of approximately 20 km were instrumentally recorded [22]. The property loss in the Assam region was more than that of the Shillong earthquake of 1897. It was followed by many aftershocks having magnitude 6.0 and above.

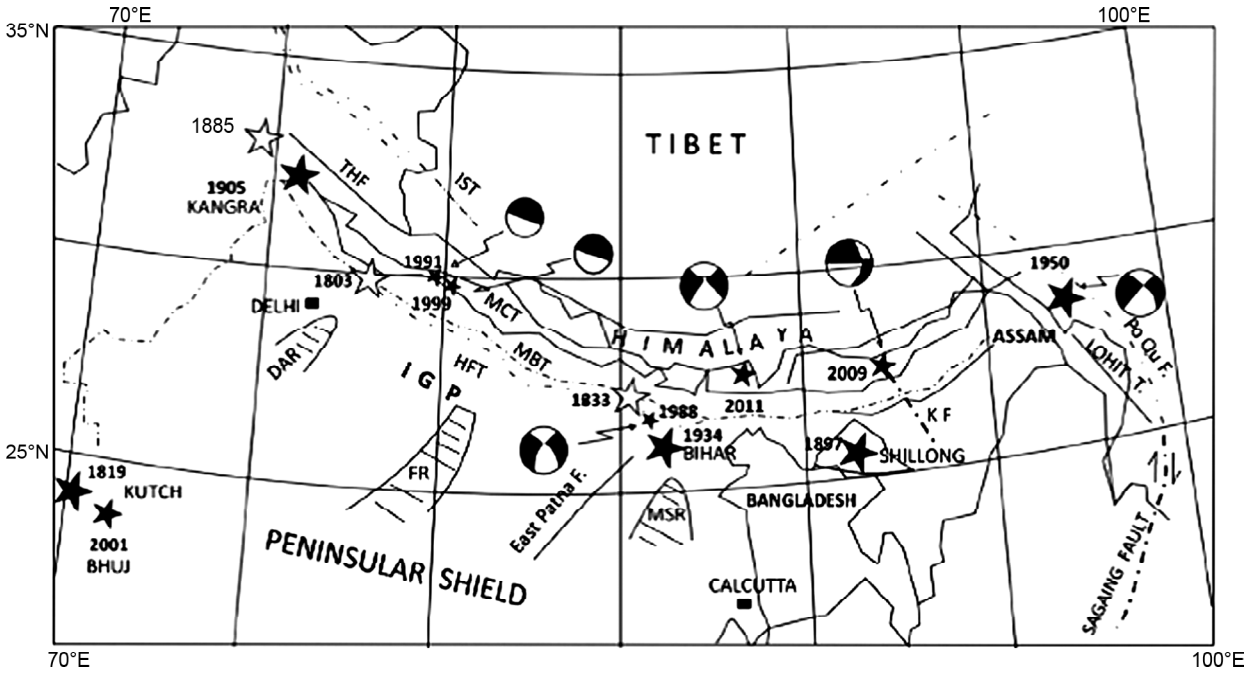

Figure 2. Map showing great earthquakes in India (bigger black stars). Smaller black stars show the recent strong earthquakes (1988, 1991, 1999, 2009 and 2011). Subsurface Ridges, FR: Faizabad Ridge; DAR: Delhi-Aravalli Ridge; MSR: Mungher Saharsa Ridge [24].

Also, apart from great earthquakes, many large earthquakes of magnitude $7.0 < M < 8.0$ have emerged from the Himalayas, namely, Central Himalayan earthquake (1505), Kumaon earthquake (1720), Satluj earthquake (1751), Garhwal - Mathura earthquake (1803), Nepal earthquake (1833), and Kashmir earthquake (2005) [23].

4. Indo-Gangetic Plains (IGP)

The Indo-Gangetic Plains (approximately between longitude 77°E -88°E and latitude 24°N-30°N) lies in between the Himalayas and the Indian Shield and covers an area of about 250,000 km^2 and is among the largest alluvial deposits in the world. The alluvial deposition is laid over a deep trough formed by the solid rock of the earth's crust ranging from 1 to 6 km [25]. In the north of Indo-Gangetic Basin (IGB), 3-4 km of thickness is seen, while, in south of IGB, the thickness is about 0.5 to 1 km. Also, in the eastern part of IGB, the thickness varies to about 2-2.5 km. IGP consists primarily of three alluvial deposits, namely, Ganga plain, Sindhu plain and Brahmaputra plain. Ganga plain have a great variation in width lying between 200-450 km and the length is about 1000 km. The Indo-Gangetic Basin is under a risk of seismic hazard as it lies very close to Himalayan belt.

The urban population of the Indian portion of IGP from Punjab to Assam is approximately 125 million (www.censusindia.gov.in). Earthquake is the most dangerous natural hazard for such a highly populated urban area. Many moderate to great earthquakes have occurred in the proximity of the Indo-Gangetic Plain, namely, Garhwal earthquake of Mw 8.0 (1803), Dhubri earthquake of Mw 7.1 (1930), Bihar-Nepal earthquake of Mw 8.1 (1934), Bihar-Nepal earthquake of Mw 6.8 (1988). If an earthquake of Mw = 8.0 occurs in future, it will cause at least 0.3 million people to be killed [26]. The large urban population in IGP is under serious threat because the fault slipping along the Himalayan thrust lines can cause massive earthquake in this region. In addition to seismicity, IGP geomorphological features such as soft and thick alluvial deposition as well as basin morphology that intensify the seismic hazard due to its high amplification potential for ground motion. The recent earthquake in Nepal (April 25, 2015, Mw 7.8) has its epicenter in the central seismic zone. Additionally, an earthquake can occur due to a slip along any of the cracks on the Indian Plate beneath the basin. These regions are classified as high seismic hazard zone (Zone IV and V) in the Indian Standard Code of Practice for Earthquake-Resistant Design of Structures IS 1893 (Part-1): 2002, due to the high seismicity of the

Himalayas and its foredeep. Design of structures on soil depend on several strong ground motion parameters, such as, ground response frequency, peak ground acceleration (PGA), peak ground speed (PGV), peak ground displacement (PGD) etc. It is therefore extremely necessary to estimate the ground motion amplification potential of IGP in order to build a safe habitat in this region.

Many other factors other than the Himalayan seismicity and IGP are responsible for the basin's seismic hazard. The interaction with the medium adds to the seismic wave amplification and thus increasing the Himalayan foredeep region's vulnerability. The inclined and vertical trough boundaries, formed by the central India plateaus, the Himalayan mountain and bend in the Indian Plate, generates surface waves by interacting with the body wave causing the "basin effect."

Moreover, the impedance contrast (between sediment and crust) is observed along the vertical direction due to the thick deposition of alluvial sediments over the hard crust. The heterogeneity in the sediment's mechanical material properties produces vertical impedance contrast between different strata causing the "stratigraphic effect." Both of these effects are responsible for altering the frequency content of strong ground motion at the surface either by attenuating or amplifying the seismic waves.

After the Mexico City earthquake (1985) and the Loma Prieta earthquake (1989) both of these effects (basin effect and stratigraphic effect) were extensively examined by seismologists [27-29]. Many researchers in India have reported the ground motion amplification characteristics of IGP. The site effect near Delhi was studied by using a two-dimensional mathematical model and the study reported in amplification of strong ground motion up to 6-7 times in the Delhi region [30]. In another study of central part of IGP, the amplification in PGA and PGV was observed up to 2-4 times and 6-12 times, respectively with the help of broadband data [31]. The site amplification in Guwahati was determined by using the bore log data alluvial deposits [32]. Figure (3) shows the geotectonic setup consisting of various tectonic features of 6° X 6° area, which is bounded by latitudes 26.9°N and 32.9°N and longitudes 74.9°E and 80.9°E.

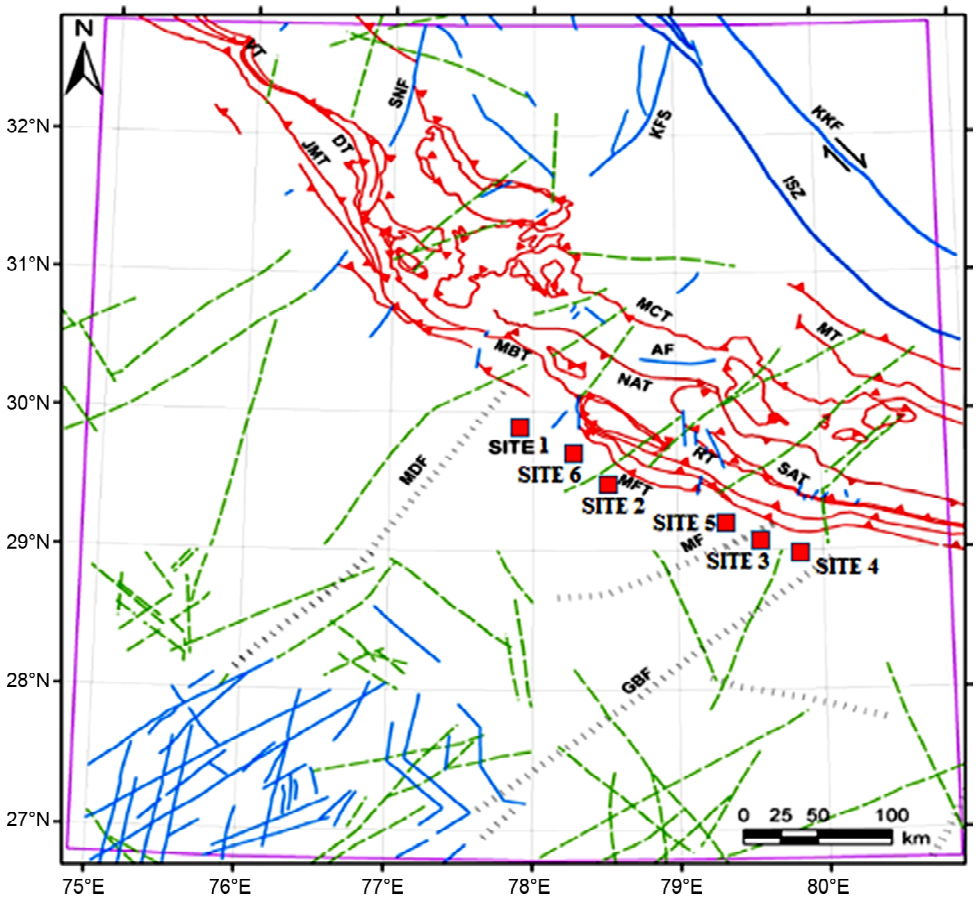

Figure 3. Geological tectonic setup in the region and the sites considered.

5. Important Cities for Case Study

All the cities selected in IGP fall in Uttarakhand state of India. Nevertheless, the State of Uttarakhand has not experienced a major earthquake (Mw $\geq$ 8.0) for more than 200 years and thus the continual accumulation of strain is due for release in this region. Therefore, the area is shown to be in the seismic gap of major earthquakes in 1934 and 1905 [33]. Because smaller earthquakes do not occur frequently enough to accommodate the observed convergence of Indian and Eurasian plates, there is a buildup of a progressive strain recognized as seismic gaps [34]. Thus, the entire state of Uttarakhand has accumulated possible slip in the seismic gap to generate future major earthquakes [35]. Hence, after being identified as a potential area for a future catastrophic earthquake is a cause of concern to all cities of this region. The cities selected for the present study are as follows:

- Roorkee (Site 1): Location of the site is latitude 29.8543°N and longitude 77.8880°E. It is a small city lying in high seismic zone IV about 180 km from New Delhi. The city is spread over a flat terrain under Sivalik Hills of Himalayas. It is situated on the banks of Ganges Canal, which flows from north-south through middle of the city.
- Kashipur (Site 2): Location of the site is latitude 29.2104°N and longitude 78.9619°E and falls in seismic zone IV. It is a city falling in Udham Singh Nagar district and Kumaun's third most populous city. The city is situated about 180 km north-west of New Delhi. Kashipur is situated in the south-west of the Kumaon region of Uttarakhand in the Terai, an area of relatively low land between 500 and 1000 feet (150 and 300 meters) above sea level and crossed by the basins of the rivers Ramganga and Kosi.
- Udham Singh Nagar (Site 3): It is a district in northern India and location of the site is latitude 28.9610°N and longitude 79.5154°E. It is located in the Terai region and is a part of Kumaon Division. From Figure (3), it can be seen that the city lies close to the Great Boundary Fault (GBF) and the Main Frontal Thrust (MFT).
- Khatima (Site 4): Location of the site is latitude 28.9209°N and longitude 79.9696°E. It is a town having an average elevation of 299 metres in Udham Singh Nagar district. The site is situated over the Great Boundary Fault (GBF) (Figur 3).
- Haldwani (Site 5): Location of the site is latitude 29.2183°N and longitude 79.5130°E and is situated in the immediate foothills of Kumaon Himalayas on the banks of Gaula river with average land elevation is 424 m above sea level. According to the Bureau of Indian Standards, haldwani falls under seismic zone IV.
- Kotdwar (Site 6): It is a municipal corporation and tehsil in Pauri Garhwal district and its location is latitude 29.7524°N and longitude 78.5269°E. The city is situated on the banks of river Khoh. The site falls in a close proximity of Main Frontal Thrust (MFT) (Figure 3).

The inset shows the area as: MBT Main Boundary Thrust. MCT Main Central Thrust, NAT North Almora Thrust. AF Alaknanda Fault. SAT South Almora Thrust. DT Drang Thrust. KFS Kaurik Fault System. GBF-Great Boundary Fault. MDF Mahendragarh Dehradun Fault.

6. Seismic Site Characterization

Shear wave velocity is an important parameter for understanding the dynamic behavior of soil. Moreover, it can be used for the determination of shear modulus (G) of soil as well as for the site characterization applications of geotechnical earthquake engineering. Six sites in IGB having a deep bedrock depth are explored using geophysical methods. Figure (3) shows the considered sites for characterization.

In the field set up, two tests were performed, firstly, active MASW consisting of Soil Spy Rosina as a data acquisition system and secondly, HVSR of Microtremor was performed in which Tromino was used as a data acquisition system. The set up used for investigating the subsurface materials for upper layers consisted of nine sensors with 2 m inter geophone spacing. For setting out a trigger, first geophone from the source was used. For HVSR analysis, this instrument has been used to record ambient vibrations for 20 minutes at each location. Grilla software [36] is used for the analysis of the data recorded in the field using Soil Spy Rosina and Tromino. After obtaining both the curves, i.e., dispersion curves and HVSR curves, Join Fit module in the Grilla software is utilized where both

the curves are placed together simultaneously for the estimation of shear wave velocity profile of deeper layers of soil.

For seismic site classification, time averaged shear wave velocity in the upper 30 m (VS30) is used as proposed by Dobry et al. [37]. The V_{S30} is estimated as follows:

$$V_{S30} = \frac{30}{\sum_{i=1}^{m} \frac{H_i}{V_{Si}}} \quad (1)$$

where, H_i shows the thickness of layer *i*, *m* is the number of layers in upper 30 m of soil and V_{Si} is the shear wave velocity of layer *i*. The classification of sites is based as per National Hazard Reduction Program (NEHRP). For site class A (V_{S30}>1500 m/s), Site class B (760 <V_{S30}<1500 m/s), Site class C (360 <V_{S30}< 760 m/s) and for Site class D (180 <V_{S30}> 360 m/s). Table (1) shows the estimated shear wave velocity of all the sites with site classification.

Figure (4) shows the graphical representation of shear wave velocity profile of all the sites where vertical axis represents the estimated depth (m) and the horizontal axis represents the shear wave velocity V_S (m/s). As expected and seen from the Figure, the shear wave velocity increases as depth increases. The estimated shear wave velocity (V_{s30}) of Roorkee is 267 m/s with engineering bedrock at a depth of around 300 m. In Kashipur, the estimated shear wave velocity (V_{s30}) is 282 m/s and engineering bedrock at a depth of 154 m. In the case of UdhamSingh Nagar, estimated shear wave velocity (V_{s30}) is 244 m/s having 160 m engineering bedrock depth. The estimated shear wave velocity (V_{s30}) in Khatima is 338 m/s having engineering bedrock depth around 150 m. The above sites inhibit lower values of shear wave velocity ranging from 240-340 m/s and falls in Site Class D according to NEHRP.

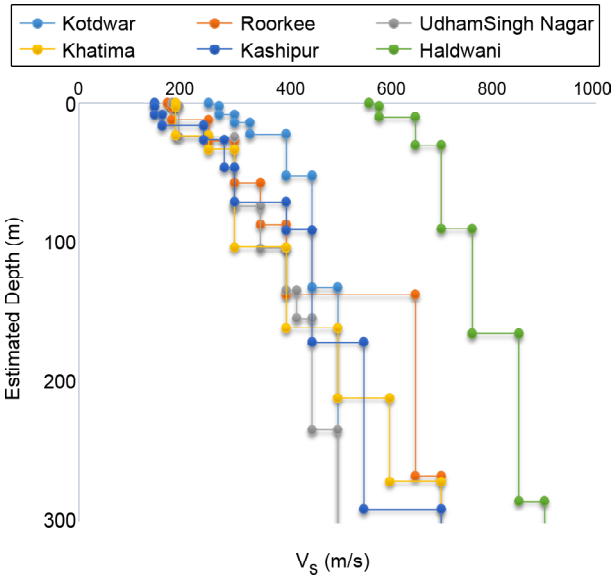

Figure 4. Shear wave velocity (Vs) profiles of all the sites.

The dominant period in the region is more than 1 s indicating the presence of thick soil cover. In Haldwani, the estimated shear wave velocity (Vs30) is 672 m/s having shallow engineering bedrock depth of 20 m, while in Kotdwar, the estimated shear wave velocity (Vs30) is 490 m/s with the engineering bedrock depth at 130 m. Both of these sites falls in site class C according to NEHRP.

7. Seismic Hazard Assessment for a Scenario Earthquake

Engineering seismology and the plate tectonics theory elaborated the understanding on earthquakes and in earthquake hazard prediction on a regional scale. However, implementation of hazard mapping at regional scale is poor in India due to its large population and application of inappropriate construction methods. Thus, in order to reduce the seismic hazard, evaluation of hazard at regional scale is required. Since 1950, no great earthquakes have been reported in the Himalayas, and thus, there is a great possibility of anytime occurrence of such an

Table 1. Estimated shear wavevelocity (V_{s30}) of sites considered.

Site	Site Name	Latitude	Longitude	Shear Wave Velocity (V_{s30})	Site Class
Site 1	Roorkee	29.8543° N	77.8880° E	267	D
Site 2	Kashipur	29.2104° N	78.9619° E	282	D
Site 3	UdhamSingh Nagar	28.9610° N	79.5154° E	244	D
Site 4	Khatima	28.9209° N	79.9696° E	338	D
Site 5	Haldwani	29.2183° N	79.5130° E	672	C
Site 6	Kotdwar	29.7524°N	78.5269°E	490	C

earthquake. Thus, there is a great need to estimate the strong ground motions for the occurrence of any seismic event in future and seismologists and earthquake geotechnical engineers are continuously working on this problem. The study of scenario earthquake will be of very much help for geotechnical earthquake engineers to establish the preparedness levels among the mass. Moreover, considering the past seismicity of the region, scenario earthquake will help in the estimation of structural damage, economic or social losses leading to the formation of Disaster Risk Management (DRM) plans.

Ground Motion Prediction Equations (GMPEs) are developed in order to predict the strong ground motion and its associated uncertainty at a particular location, which depends on many factors, such as, magnitude of an earthquake, distance of the source-to-site, fault mechanism and local soil conditions, etc. These GMPEs are being efficiently used in the estimation of ground motions in seismic hazard analysis.

In the present work, PEER NGA West 2 models are used to estimate the strong ground motion of the study region. These models are globally used for PGA, PGV and ordinates of the response spectrum calculation by using various input parameters. These models have the capability of ground motion prediction for shallow crustal earthquakes for different ranges of magnitude, site conditions and distances. These GMPEs are referred to as ASK14 [38], BSSA14 [39], CB14 [40], CY14 [41], and I14 [42]. In these GMPEs, NGA-West 2 database is widely expanded by the inclusion of more than 20,000 recordings obtained from Californian earthquakes (M<5.5) and also from other sources of active tectonic regions (M>5.5). All the models use the Rrup defined as the distance closest to surface of fault rupture, except BSSA 14 in which R_{jb} is used for ground motion calculations. The parameter *Z*1.0, defined as the depth where shear wave velocity (*Vs*) is 1 km/sec below the site is used in BSSA14, ASK14 and CY14 GMPEs for the modeling of basin effects and sediment-depth. However, in CB14 GMPE, the modeling of these effects is carried out by the parameter Z2.5, defined as the depth where shear wave velocity (*Vs*) is 2.5 km/sec below the site. In these GMPEs, the default values set by the developers for Z1.0 and Z2.5 is used. In this study, BSSA 14 GMPE is used for the calculation of strong ground motion, in which, the applicable range of magnitude (*M*) lies between 3.0 to 8.5, the Rjb varies from 0 to 400 km and the range of shear wave velocity varies from 150 m/s to 1500 m/s for 0.01-10s spectral periods. The source regional variability, site effects and path effects are included in this model. The ground motion is predicted from the following equation:

$$\ln Y = F_E(M, mech) + F_P(R_{JB}, M, region) + F_s(V_{S30}, R_{JB}, M, region, z_1) + \varepsilon_n \sigma(M, R_{JB}, V_{S30}) \quad (2)$$

where ln *Y* denotes the predicted ground motion i.e. PGA, PGV; F_E represents the source function; F_P represents the path function and FS represents the site effects function; σ represents the standard deviation of the model; σ_n is the number in fraction of standard deviation in the case when ln *Y* is away from the mean value, while, *M*; R_{JB} (km); *mech*; *region*; z_1 (km) and V_{S30} (m/s) are all predictor variables of the model.

The response of sites in Indo-Gangetic Basin in dynamic conditions are studied for a scenario earthquake of magnitude Mw = 8.0. It is assumed that the event has occurred at Himalayan Frontal Thrust (HFT). The top of the fault is assumed to be at 0 km depth with angle of dip taken as 450. The width of the fault is taken as 21 km and shear wave velocity is estimated from the geophysical methods. The fault has reverse mechanism and the sites are located on the hanging wall side.

8. Results and Discussions

Figure (5) shows the variation of spectral acceleration with the time period of two sites, Haldwani and Roorkee. It can be observed from the figure that low spectral acceleration in Haldwani as compared to Roorkee is seen due to shallow bedrock depth in Haldwani and deep soil in Roorkee. Moreover, the maximum spectral acceleration in Haldwani is around 3.3 sec while it shifts to around 5.5 sec in case of Roorkee. This is due to the increase in soil thickness in the latter. Thus, the structures with long time period will be most affected in case of seismic event in Roorkee, while, short time period structures will be affected in Haldwani due to the resonance.

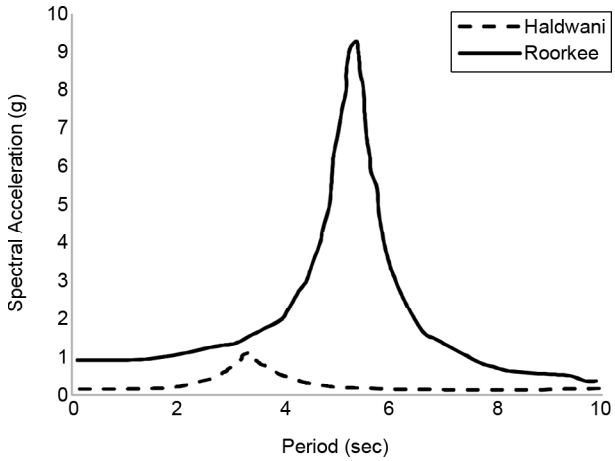

Figure 5. Response spectra of sites Haldwani and Roorkee.

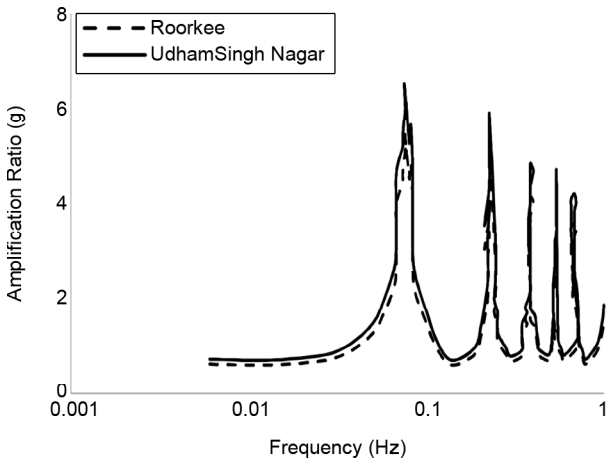

Figure 7. Amplification ratio for Roorkee and UdhamSingh Nagar.

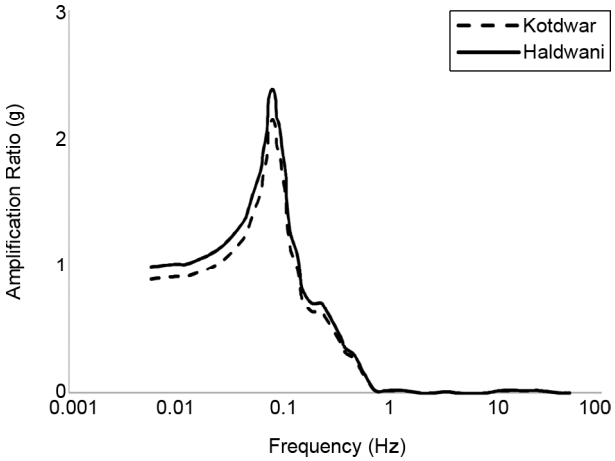

Figure 6. Amplification ratio for Kotdwar and Haldwani.

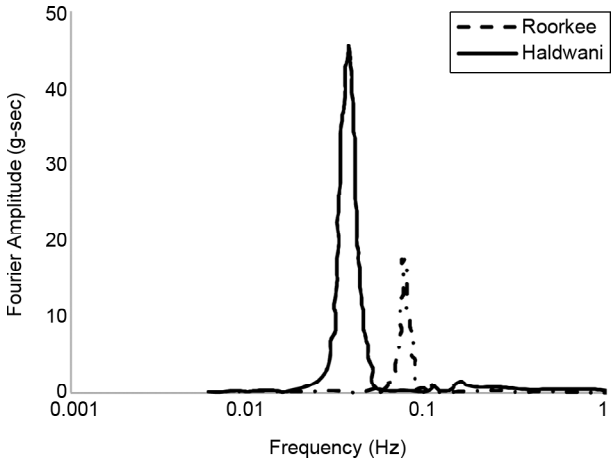

Figure 8. Fourier Amplitude Spectra for Roorkee and Haldwani.

Figure (6) shows the variation of amplification ratio versus the frequency for two sites, namely, Kotdwar and Haldwani having shallow bedrock depth. The amplification ratio is comparatively less for Haldwani as observed from the figure. The dominant frequency is about 0.1 Hz.

For sites with deep bedrock depth i.e. Roorkee and UdhamSingh Nagar, Figure (7) shows the variation of amplification ratio. It can be observed that the amplification ratio is 7.0 for Roorkee, while around 6.0 for UdhamSingh Nagar. This increase in amplification is due to the presence of thick soil cover in these region. Initially, there is an increase in amplification with increase in thickness of soil and further reaches to saturation. Moreover, there is a shift in the predominant frequency of strong ground motion to the lower side as compared to Figure (6).

Figure (8) represents the Fourier spectra corresponding to surface ground motions for two sites, namely, Roorkee having deep soil and Haldwani having shallow bedrock depth. It can be seen from Figure (8) that there is a shift in predominant frequency to lower side with the increase in soil thickness as compared to Haldwani. Also, there is a huge difference in the Fourier amplitude of both sites.

9. Probabilistic Seismic Hazard Assesement (PSHa)

The division of the study area into seismic zones having individual characteristics, is one of the fundamental requirements for the estimation of seismic hazard parameters. As discussed in earlier section, the entire Himalayan region (20°-36°N and 69°-100°E) is seismically very active and seismotectonically highly complicated. The entire study region is divided into seven seismic zones based on seismotectonics, seismicity distribution, and to pographic variations as shown in Figure (9). A brief description about all of the seven seismogenic source zones is given below:

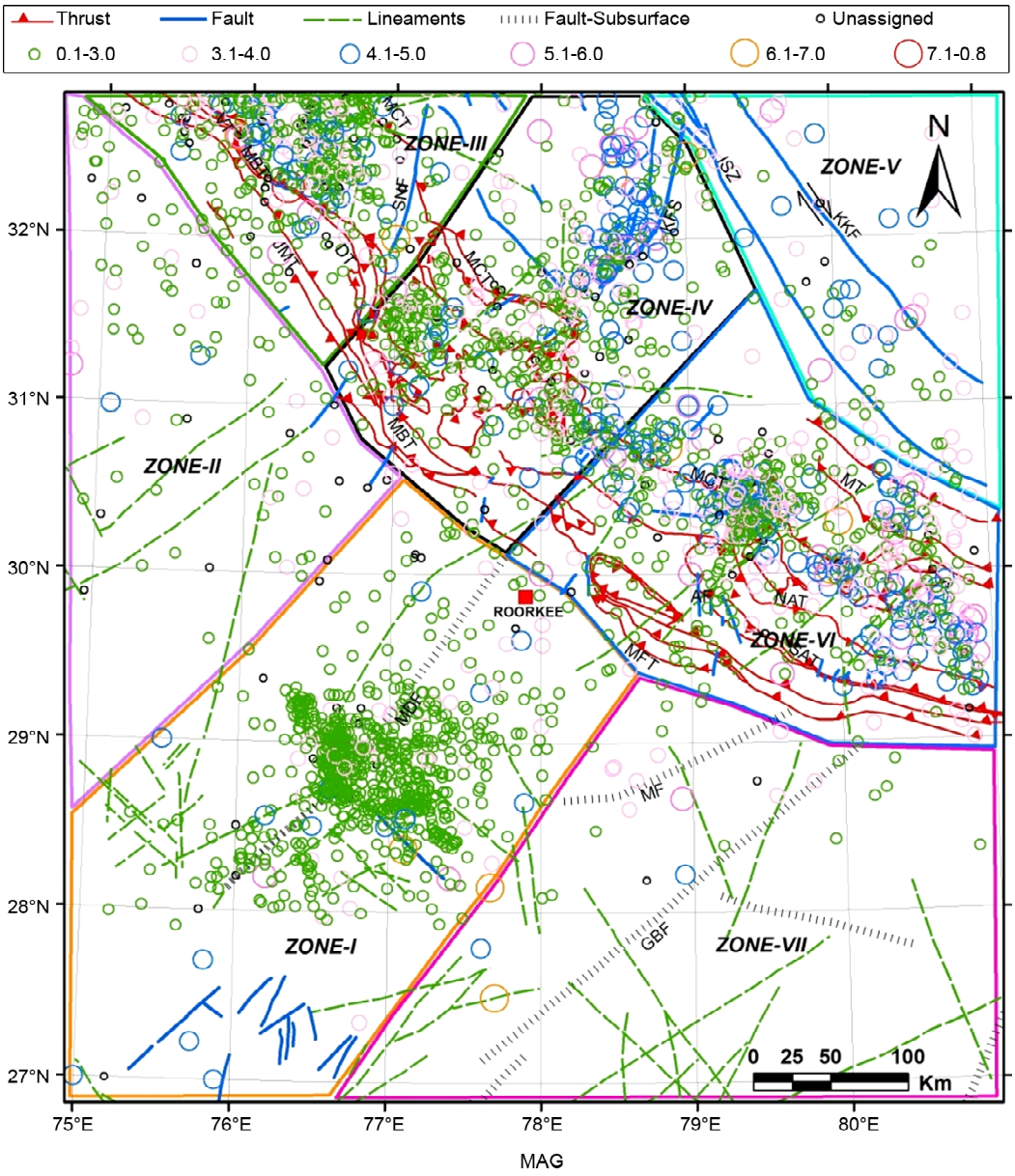

Figure 9. Division of study area into seven seismogenic source zones.

9.1. Seismogenic Zone-I

Seismogenic zone-I consists of a prominent tectonic feature of the NNE trending subsurface Mahendragarh Dehradun Fault (MDF) extending northeast to the foothills of the Himalayas. The Delhi-Hardwar ridge is associated with the MDF and is considered to be an extension of the Peninsular Rock (Aravalli). In the the eastern boundary of the tectonic province of Delhi-Moradabad lies the Moradabad fault zone. This area is very seismically active and with varying earthquakes magnitude from 1.1 to 6.5 and 1 to 109 km in depth.

9.2. Seismogenic Zone-II

This zone comprises of the western parts of Indo-Gangetic basin. This zone is composed of alluvium and is identified by NE-SW and NW-SE trending lineaments. The variation in earthquakes magnitude ranges from 2.0 to 5.5 and variation in depth ranges from 4 to 145 km.

9.3. Seismogenic Zone-III

This zone is the northwest portion of the structural belt of the Himalayas. In this part, the Himalayan structural trend is mostly NW-SE and is affected by Sundernagar Fault's transverse faults in the east. The major tectonic features in this zone are, namely, Main Central Thrust (MCT), Main Frontal Thrust (MFT), Main Boundary Thrust (MBT), and Sundernagar Fault (SNF). The occurrence of

earthquakes in this zone is very high, particularly in the area between the MBT and MCT signaling severe tectonic activity in the region. The earthquakes in this zone range from 1.6 to 8.0 in magnitude and 1 to 225 km in depth.

9.4. Seismogenic Zone-IV

This zone consists of the Himalayan belt of eastern part of Himachal Pradesh and western part of Uttarakhand. The Himalayan structural trend is mostly NW-SE in this zone. The major tectonic features in this region are Main Central Thrust (MCT), Main Boundary Thrust (MBT), North Almora Thrust (NAT) and Main Frontal Thrust (MFT). The neotectonic Kaurik Fault System (KFS) defined by the number of half-graben faults is very active and is considered to have triggered the Kinnaur earthquake of 1975 [43]. Moreover, Uttarkashi earthquake of 1991 also occurred in this zone. The range of earthquakes magnitude in this zone varies from 1.2 to 6.6 and depth range from 1 to 169 km.

9.5. Seismogenic Zone-V

This zone consists of the Trans-Himalayan region and is marked by the Indus Suture Zone (ISZ) and extensive Karakoram Fault (KKF). ISZ marks the boundary between the Indian and Tibetan plates. KKF is the most extensive tectonic feature that has affected the region with a huge dextral offset and is traceable to the Pamir in the northwest through the Shyok Suture. It extends from Central Pamir to Kumaon Himalayas up to 1000 km. This zone consists of deep marine Triassic to Eocene sediments acquired from the Neotethyan oceanic crust. The range of earthquakes magnitude in this zone varies from 2.3 to 6.0 and depth range from 3 to 155 km.

9.6. Seismogenic Zone-VI

In this zone, Himalayan belt of Uttarakhand and westernmost part of Nepal exists having NW-SE trend towards west and then changes to east of southeast. The major tectonic features in this zone are, namely, Main Central Thrust (MCT), Martoli Thrust (MT), southward dipping North Almora Thrust (NAT), Main Boundary Thrust (MBT), South Almora Thrust (SAT), Main Frontal Thrust (MFT) and Ramgarh Thrust (RT). However, longitudinal E-W trending Alaknanda fault and other transverse faults highly affect this zone. Moreover, in this zone, significant earthquake clusters are located across MCT and to the north of MBT. Thus, marking the area between MBT and MCT to be seismically very active. The Chamoli earthquake (1999) occurred in this zone. The range of earthquakes magnitude in this zone varies from 1.2 to 6.8 and depth range from 1 to 114 km.

9.7. Seismogenic Zone-VII

This zone comprises of the NE-SW trending Great Boundary Fault (GBF) and Moradabad Fault (MF) and few lineaments. In Delhi-Moradabad province, Moradabad fault forms the boundary between Neogene and the Delhi basement. The range of earthquakes magnitude in this zone varies from 1.6 to 6.7 and depth range from 2 to 58 km.

10. Hazard Parameters Determination

The available earthquake catalogues usually consist of two types of information, i.e. macroseismic observations of major seismic events that occurred over a period of a few hundred years, and the other, instrumental data for comparatively short period of time. Methods commonly used to estimate seismic activity parameters (parameter b in G-R equation, M_{max} and earthquake activity rate, I) are not appropriate for this type of data because of the incompleteness of macroseismic part of the catalogue. Kijko and Sellevoll [44]developed a method using both the information on strong events contained in the macro-seismic part of the catalogue and the information contained in the complete catalogue containing complete data above a certain magnitude threshold.

In the present study, the above approach is used to estimate seismic hazard parameters in seven major seismotectonic zones (seismic zones) of the Himalayas. Also, in this approach, the complete part of the catalogue is being used.

11. Data Files and Computational Remarks

The earthquake catalogue (1720-2018) was compiled in this study by extracting data from different sources, namely, India Metrology Department (IMD, Indian agency), International Seismological Center (ISC, UK) and United States

Table 2. Input Data for seismic hazard estimation.

Seismic Zone	Threshold Magnitude	Mc	Standard Deviation	Max. Observed Magnitude
I	5.0	3.1	0.3	6.5
II	5.0	3.4	0.3	5.5
III	5.0	3.5	0.3	8.0
IV	5.0	3.6	0.3	6.6
V	5.0	3.1	0.3	6.0
VI	5.0	3.2	0.3	6.8
VII	5.0	2.9	0.3	6.7

Geological Survey (USGS, USA) (International agencies). Moreover, available literature on earthquakes in India in various national and international publications and journals has also been used for compilation of the data. A widely known approach [44] is used for the estimation of seismic hazard parameters for the complete data files. For each seismic source zone, to estimate the seismic hazard, it was assumed that the maximum magnitude M_{max} was determined with the standard error as 0.10 having threshold magnitude 5.0. M_c is defined as the lowest magnitude at which 100% of the events in a space-time volume is detected. Below M_c, a fraction of events is missed by the network because they are too small to be recorded on enough stations. Table (2) presents the summary of the input parameters of seven seismic zone for the estimation of seismic hazard.

12. Results and Discussions

In seismology and studies related to earthquake prediction, the most important parameter in the G-R relation is the parameter *b*. This parameter is an indication of various mechanical properties, namely, crack density, stress concentration and degree of heterogeneity in the seismogenic materials. Table (3) represents the estimated hazard parameters (λ, β, *b* value and M_{max}) for all the seven seismic zones of the study region. From the Table (3), on a regional scale, the *b* value is relatively high for seismic zone VI indicating high locally concentrated stress and fracturing. The *b* value is quite different from one seismic zone to another. It can also be observed from the Table (3), that, β value decreases from seismic zone I to seismic zone *V* and then increases again in seismic zone VI and further decreases in seismic zone VII. Consequently, *b* value also follows the same trend as that of β. Moreover, the value of λ is highest in seismic zone IV and lowest in seismic zone II. For $m \geq 6.0$, the estimated return periods in seismic zones I, II, VI and VII are higher than the return periods of seismic zones III, IV and V, implying that the seismic zones III, IV and V are more prone to occurrence of strong events than seismic zones I, II, VI and VII. Hence, considering the estimated return periods for $R_{6.0}$, $R_{7.0}$ and $R_{8.0}$, it can be stated that the seismic zone IV is the most active in the whole region.

As per the current Indian code of practice, IS 1893 (Part-I): 2017 [11] the study area lies in zone IV of seismic hazard level. This corresponds to a PGA value of 0.24 g for MCE scenario. Attributing to region of high seismicity, many researchers in this area have performed the seismic hazard assessment [45-46]. The seismic hazard assessment for the whole Indian region is reported under the global seismic hazard assessment program [47] and PGA reported for Dehradun city (70 km from Roorkee city) corresponding to 10% exceedance probability in 50 years is between 0.1 to 0.3 g. The corresponding value as proposed by Mahajan et al. [46] is 0.3-0.4 g for the same exceedance probability. Nath and Thingbaijam [48] predicted a PGA value of 0.47 g for MCE for Dehradun city. Table (4) presents a comparison of the PGA value for 10% probability in 50 years for all the six sites

Table 3. Estimated seismic hazard parameters for the present study.

Seismic Zone	λ	β	b Value	M_{max}	$R_{6.0}$	$R_{7.0}$	$R_{8.0}$
I	1.69±0.20	1.84±0.30	0.80±0.13	7.0±0.35	123	776	4898
II	0.18±0.17	1.81±0.02	0.79±0.01	6.0±0.40	617	3802	23442
III	0.92±0.14	1.63±0.70	0.71±0.32	8.5±0.25	65	331	1698
IV	4.48±0.20	1.56±0.71	0.68±0.31	7.1±0.50	10	46	219
V	1.21±0.16	1.49±0.27	0.65±0.12	6.5±0.48	63	282	1259
VI	1.42±0.15	1.91±0.32	0.83±0.14	7.3±0.37	148	1000	6761
VII	0.78±0.17	1.70±0.00	0.74±0.00	7.2±0.30	251	1380	7586

Table 4. Estimated PGA value for 10% probability in 50 years for the considered sites.

Site Name	Nath and Thingbaijam [48]	Mahajan et al. [46]	Present Study
Roorkee	0.30-0.35	0.30-0.40	0.35-0.38
Kashipur	0.25-0.30	0.30-0.35	0.28-0.32
UdhamSingh Nagar	0.20-0.30	0.15-0.25	0.21-0.24
Khatima	0.22-0.26	0.15-0.20	0.20-0.22
Haldwani	0.15-0.20	0.15-0.25	0.18-0.23
Kotdwar	0.15-0.20	0.15-0.25	0.17-0.21

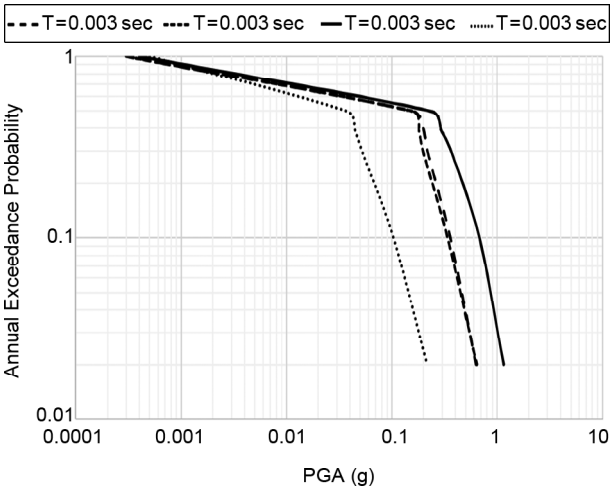

Figure 10. Hazard curve at bedrock for Roorkee city.

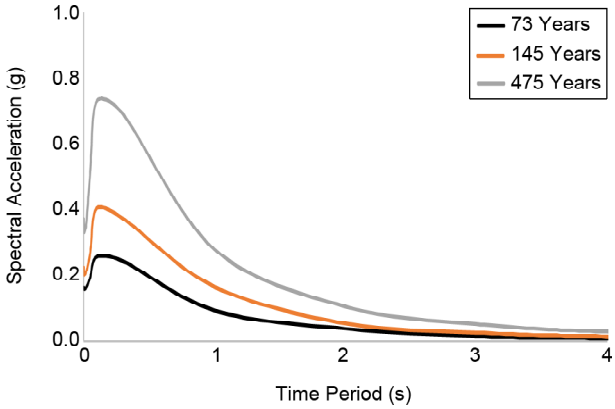

Figure 11. Response spectra for Roorkee city (Site Class D) for different structural periods.

considered in the study with the results obtained from Mahajan et al. [46] and Nath and Thingbaijam [48]. The present value seems higher than the results of Bhatia et al. [47]and possibly in agreement with Nath and Thingbaijam [48] and Mahajan et al. [46].

The hazard curve for the Roorkee city is shown in Figure (10) for four spectral periods at $T=0.003$ sec, $T=0.02$ sec, $T=0.3$ sec and $T=2$ sec. It can be observed from the figure that the exceedance probability decreases with the increase in spectral acceleration. The strong motion prediction has been carried out for five return periods (73, 100, 145, 475 and 2475 years) and for ten spectral periods (0.03, 0.05, 0.1, 0.2, 0.3, 0.5, 1, 2, 3, and 4 seconds). Figure (11) shows the response spectra for Roorkee city for three return periods, i.e., 73 years, 145 years and 475 years.

13. Conclusions

One of the most challenging issues in assessing seismic hazards is predicting deep soil effects at a given site in case of any seismic event. Deep soil effects for seismic design should be considered as variation in mechanical characteristics is observed with the increase in thickness of the soil. Seismic site characterization of six important cities in the state of Uttarakhand (Seismic Zone IV) is carried out using geophysical methods. Four sites fall in site class D and two sites in site class C according to NEHRP. The response of sites in Indo-Gangetic Basin in dynamic conditions are studied for a scenario earthquake of magnitude $M_w = 8.0$ and high spectral acceleration is observed for deep soil profiles as compared to shallow soil profiles. The increase in amplification is observed due to the presence of thick soil cover in the region. Initially, there is an increase in amplification with increase in thickness of soil and further reaches to saturation. The amplification ratio ranges from 1.0 to 7.0 in deep soil profiles while it ranges from 1.0 to 2.5 in shallow soil profiles. Moreover, shift in the predominant frequency of strong ground motion is seen towards the lower side in the case of deep soil profiles.

Moreover, an endeavor is made to compute peak ground horizontal accelerations at bedrock level for all the six sites due to the presence of seismogenic sources present around them. The study area is divided in seven seismogenic sources for the estimation of seismic hazard assessment using the complete

part of seismicity data. The *b* value is quite different from one seismic zone to another. On a regional scale, the b value is relatively high for seismic zone VI indicating high locally concentrated stress and fracturing. Also, the value of λ is highest in seismic zone IV and lowest in seismic zone II. For $m \geq 6.0$, the estimated return periods in seismic zones I, II, VI and VII are higher than the return periods of seismic zones III, IV and V, implying that the seismic zones III, IV and V are more prone to occurrence of strong events than seismic zones I, II, VI and VII. Hence, considering the estimated return periods for $R_{6.0}$, $R_{7.0}$ and $R_{8.0}$, it can be stated that the seismic zone IV is the most active in the whole region. A comparison of the PGA value for 10% probability in 50 years for all the six sites considered in the study with the results obtained from Mahajan et al. [46] and Nath and Thingbaijam [48]. The present value seems higher than the results of Bhatia et al. [47] and possibly in agreement with Nath and Thingbaijam [48] and Mahajan et al. [46]. Hence, the estimated hazard parameters, probability of occurrence and return periods may be considered as quantitative measures of seismicity and for preparation of microzonation maps for the study region. Seismic characteristics of seismogenic source zones may be used for earthquake engineering purposes for assigning the severity of region for earthquake resistant construction.

References

1. Phanikanth, V.S., Deepankar Choudhury, and Rami Reddy, G. (2011) Equivalent-linear seismic ground response analysis of some typical sites in Mumbai. *Geotechnical and Geological Engineering*, **29**(6), 1109-1126.

2. Kumar, A., Anbazhagan, P., and Sitharam, T.G. (2012) Site specific ground response study of deep indo-gangetic basin using representative regional ground motions. *GeoCongress*, Oakland, USA, March.

3. Jishnu, R.B., Naik, S.P., Patra, N.R., and Malik, J.N. (2013) Ground response analysis of Kanpur soil along Indo-Gangetic plains. *Soil Dyn. Earthq. Eng.*, **51**, 47-57.

4. Luke, B.A., Matasovic, N., and Kemintz, M. (2001) Evaluating seismic response of deep sandy soil deposits. *Bull. Seismolog. Soc. Am.*, **91**, 1516-1525.

5. Ashford, S.A., Jakrapiyanun, W., and Lukkunaprsit, P. (2007) Amplification of earthquake ground motions in Bangkok. *Proceedings of the 12th World Conference on Earthquake Engineering*, Auckland, New Zealand.

6. Anbazhagan, P. and Sitharam, T. G. (2008) Site characterization and site response studies using shear wave velocity. *Journal of Seismology and Earthquake Engineering*, **10**(2), 53-67.

7. Huang, Y., Weimin, Y., and Chen, Z. (2009) Seismic response analysis of the deep saturated soil deposits in Shanghai. *Environ. Geol.*, Springer, **56**(6), 1163-1169.

8. Chen, Q.S., Gao, G.Y., and Yang, J. (2011) Dynamic response of deep soft soil deposit under multidirectional earthquake loading. E*ng. Geol.*, **121**(1-2), 55-65.

9. Jakka, R.S., Hussain, Md., and Sharma, M.L. (2015) Effects on amplification of strong ground motion due to deep soils. *Geomechanics and Engineering*, **8**(5), 663-674.

10. Abhishek, K., Olympa, B., and Harinarayan, N.H. (2016) Obtaining the surface PGA from site response analyses based on globally recorded ground motions and matching with the codal values. *Natural Hazards*, **81**(1), 543-572.

11. IS 1893 (2002) *Indian Standard Criteria for Earthquake Resistant Design of Structures, Part 1 - General Provisions and Buildings.* Bureau of Indian Standards, New Delhi.

12. Nakamura, Y. (1989) A method for dynamic characteristics estimation of subsurface using microtremors on the ground surface. *Quart. Rep. Railway Tech. Res. Inst.*, **30**(1), 25-33.

13. Yin, A. (2006) Cenozoic tectonic evolution of the Himalayan orogen as constrained by along-strike variation of structural geometry, exhumation history, and foreland sedimentation. *Earth-Science Reviews*, **76**, 1-131.

14. Bilham, R., Larson, L., and Jeffrey, F. (1997)

GPS measurements of present day convergence across the Nepal Himalaya. *Nature*, **386**, 61-64.

15. Teotia, S.S., Khattri, K.N., and Roy, P.K. (1997) Multifractal analysis of seismicity of the Himalayan region. *Current Science*, **73**(4), 359-366.

16. Kumar, S. and Mahajan, A.K. (2001) Seismotectonics of the Kangra region, northwest Himalaya. *Tectonophysics*, **331**(4), 359-371.

17. Sharma, M.L. and Lindholm, C. (2012) Earthquake hazard assessment for Dehradun, Uttarakhand, India, including a characteristic earthquake recurrence model for the Himalaya Frontal Fault (HFF). *Pure and Applied Geophysics*, **169**(9), 1601-1617.

18. Gupta, H. and Gahalaut, V.K. (2014) Seismotectonics and large earthquake generation in the Himalayan region. *Gondwana Research*, **25**(1), 204-213.

19. Middlemiss, C.S. (1910) The Kangra earthquake of 4 April 1905. *Geol. Surv. India Mem.*, **38**, p409.

20. Dunn, J.A., Auden, J.B., Ghosh, A.M., and Wadia, D.N. (1939) The Bihar-Nepal Earthquake of 1934. *Geol. Surv. India Mem.*, **73**, 205.

21. Dunn, J.A., Auden, J.B., and Ghosh, A.M.N., (1939) Discussion of scales and isoseismals. *Memoir Geological Survey of India*, **73**, 7-26.

22. Tandon, A.N. (1954) A study of Assam earthquake of August 1950 and its aftershocks. *Indian J. Meteorol. Geophys.*, **5**, 95-137.

23. Thakur, V.C. (2006) Reassessment of earthquake hazard in the Himalaya and implications from the 2004 Sumatra-Andaman earthquake. *Curr. Sci.*, **90**(8), 1070-1072.

24. Kayal, J.R. (2010) Himalayan tectonic model and the great earthquakes: an appraisal. *Geomatics, Nat. Hazards. Risk*, **1**, 51-67.

25. Wadia, D.N. (1964) The Himalaya mountains: their age, origin and sub-crustal relations. *MeghnadSaha Memorial Lecture, National Institute of Sciences of India*, New Delhi.

26. Bilham, R. (2009) The seismic future of cities. *Bulletin of Earthquake Engineering*, **7**, 839-887.

27. Chavez-Garcia, J.F. and Bard, P.Y. (1994) Site effects in Mexico City eight years after the September 1985 Michoacan earthquakes. *Soil Dynamics and Earthquake Engineering*, **13**, 229-247.

28. Ashford, S.A., Jakrapiyanun, W., and Lukkunaprasit, P. (2000) Amplification of earthquake ground motions in Bangkok. *Proc. of the 12th World Conference on Earthquake Engineering.*

29. Ferrer-Toledo, H., Chavez-Garcia, F., and Cardenas-Soto, M. (2004) Ground motion in Central Mexico. Path effects due to the Transmexican Volcanic Belt. *Proc. of the 13th World Conference on Earthquake Engineering*, 1-6.

30. Parvez, I.A., Vaccari, F., and Panza, G.F. (2006) Influence of source distance on site-effects in Delhi city. *Current Science*, **91**(6), 827-835.

31. Srinagesh, D., Singh, S.K., Chadha, R.K., Paul, A., Suresh, G., Ordaz, M., and Dattatrayam, R.S. (2011) Amplification of seismic waves in the Central Indo-Gangetic Basin, India. *Bulletin of the Seismological Society of America*, **101**(5), 2231-2242.

32. Raghukanth S.T.G., Dixit, J., and Dash, S.K. (2011) Ground motion for scenario earthquakes at Guwahati City. *Acta Geodetica et Geophisica Hungarica*, **46**(3), 326-346.

33. Yeats, R.S. and Thakur, V.C. (2008) Active faulting south of the Himalayan Front: establishing a new plate boundary. *Tectonophysics*, **453**(1-4), 63-73.

34. Bilham, R., Blume, F., Bendick, R., and Gaur, V.K. (1998) Geodetic constraints on the translation and deformation of India: implications for future great Himalayan earthquakes. *Curr. Sci.*, **74**, 213-229.

35. Khattri, K.N. (1987) Great earthquakes, seismicity gaps and potential for earthquake disaster along the Himalaya plate boundary. *Tectonophysics*,

138(1), 79-92.

36. Micromed, S.P.A. (2008) *Soil Spy Rosina User's Manual*. Ver. 2.0, Treviso, Italy.

37. Dobry, R., Borcherdt, R.D., Crouse, C.B., Idriss, I.M., Joyner, W.B., Martin, G.R., Power, M.S., Rinne, E.E., and Seed, R.B. (2000) New site coefficients and site classification system used in recent building seismic code provisions. *Earthquake Spectra*, **16**, 41-67.

38. Abrahamson, N.A., Silva, W.J., and Kamai, R. (2014) Summary of the ASK14 ground motion relation for active crustal regions. *Earthquake Spectra*, **30**(3), 1025-1055.

39. Boore, D.M., Stewart, J.P., Seyhan, E., and Atkinson, G.M. (2014) NGA-West2 equations for predicting PGA, PGV, and 5% damped PSA for shallow crustal earthquakes. *Earthquake Spectra*, **30**, 1057-1085.

40. Campbell, K.W., and Bozorgnia, Y. (2014) NGA-West2 ground motion model for the average horizontal components of PGA, PGV, and 5% damped linear acceleration response spectra. *Earthquake Spectra*, **30**(3), 1087-1115.

41. Chiou, B.S-J. and Youngs, R.R. (2014) Update of the Chiou and Youngs NGA model for the average horizontal component of peak ground motion and response spectra. *Earthquake Spectra*, **30**(3), 1117-1153.

42. Idriss, I.M. (2014) An NGA-West2 empirical model for estimating the horizontal spectral values generated by shallow crustal earthquakes. *Earthquake Spectra*, **30**(3), 1155-1177.

43. GSI (2000) *Seismological Atlas of India and Its Environs*. Geological Survey of India.

44. Kijko, A. and Sellevoll, M.A. (1989) Estimation of seismic hazard parameters from incomplete data files. Part I: utilization of extreme and complete catalogues with different threshold magnitudes. *Bull. Seismol. Soc. Am.*, **79**, 645-654.

45. Sharma, M.L. (2003) Seismic hazard in Northern India region. *Seismological Research Letters*, **74**(2), 140-146.

46. Mahajan, A.K., Thakur, V.C., Sharma, M.L., and Chauhan, M. (2010) Probabilistic seismic hazard map of NW Himalaya and its adjoining area, India. *Nat Hazards*, **53**, 443-457.

47. Bhatia, S.C., Kumar, M.R., and Gupta, H.K. (1999) A probabilistic seismic hazard map of India and adjoining regions. Annali di Geofisica, **42**(1), 153-166.

48. Nath, S.K. and Thingbaijam, K.K.S. (2012) Probabilistic seismic hazard assessment of India. *Seismological Research Letters*, **83**(1), 135-149.